

## Theoretical and experimental studies of band formation in CO adlayers

Inder P. Batra and K. Hermann\*

*IBM Research Laboratory, San Jose, California 95193*

A. M. Bradshaw and K. Horn

*Fritz-Haber-Institut der Max-Planck-Gesellschaft, Faradayweg 4-6, 1000 Berlin 33, West Germany*

(Received 27 November 1978; revised manuscript received 8 February 1979)

We have performed electronic-structure calculations using the extended tight-binding method for two-dimensional isolated layers of CO molecules corresponding to the ordered arrays formed on a Pd(100) surface. We find that the calculated width and shape of the  $4\sigma$ -derived band is in good agreement with angular-resolved photoemission results from this system. The calculated widths of the  $5\sigma$ - and  $1\pi$ -derived bands are much greater than that of the  $4\sigma$ -derived band, reflecting their more delocalized nature. In the photoemission experiment some dispersion is detected on the  $5\sigma + 1\pi$  composite level but it was not possible to separate out the component bands.

### I. INTRODUCTION

The interaction between chemisorbed molecules (or atoms) and solid surfaces is currently being studied using band-theoretical as well as cluster-model techniques. In the cluster concept, one usually considers the interaction of a single ad-particle with the surface (which is itself represented by a few atoms) thus neglecting direct or indirect interaction between different ad-particles. One obtains, as a result of such calculations, the energy location of various electronic states of the system which can be compared with conventional photoemission spectra. Clearly, the cluster is an appropriate description in the limit of vanishing adsorbate coverage. At higher coverages the adsorbed species can interact with each other both directly ("through space") and indirectly ("through substrate") and in many cases form ordered overlayers. In this case, it may be more appropriate to describe the electronic structure of the system on the basis of band models with two-dimensional periodicity. The electronic states are  $\bar{k}_{\parallel}$  dependent and the calculated dispersion can be compared to angular-resolved photoemission data.<sup>1-3</sup>

In a previous communication<sup>4</sup> we have briefly described the results of angular-resolved photoemission experiments for CO chemisorbed on Pd(100). For near saturation coverage and a defined crystal azimuth, we have found that the energetic position of the  $4\sigma$  peak of CO shows a characteristic dependence on the polar angle of emission. When translated into band-theory language this amounts to a  $\bar{k}_{\parallel}$  dispersion of about 0.4 eV. At lower coverage the  $\bar{k}_{\parallel}$  dispersion fell below the accuracy ( $\pm 0.04$  eV) of our measurements. We have since investigated the dispersion of

the composite<sup>5</sup> ( $5\sigma + 1\pi$ )-derived band.

In order to understand the shape and width of these bands, we have performed electronic-structure calculations for isolated two-dimensional ordered layers of CO molecules at different densities. Geometrical structures of the layers were chosen to represent the situation on the Pd(100) surface. Low-energy electron diffraction (LEED) studies<sup>6</sup> of the CO-Pd(100) system show that at coverages  $\Theta = 0.5-0.8$  CO forms an ordered overlayer consisting of two orthogonal domains. At  $\Theta = 0.5$ , this structure has been denoted by  $c(4 \times 2)-45^\circ$ , although a vector notation is more appropriate. With increasing coverage, a uniaxial compression of each domain in a [100] azimuthal direction occurs resulting in a hexagonal structure at  $\Theta = 1/3^{1/2} \approx 0.58$  and reaching saturation at  $\Theta = 0.8$ .

Two-dimensional band-structure calculations for the CO monolayers at  $\Theta = 0.5, 0.58$ , and  $0.8$  give a  $4\sigma$  dispersion of 0.02, 0.04, and 0.3 eV, respectively, which can be compared with the experimental results for the chemisorbed situation because the CO  $4\sigma$  orbital is not involved in the chemisorption bond with the surface. The agreement between the theoretical and experimental  $4\sigma$  bands at  $\Theta = 0.8$  is very good, even reproducing the band shape in different  $\bar{k}_{\parallel}$  directions, as will be shown in Secs. II-IV. The  $1\pi$  and  $5\sigma$  orbitals in isolated CO are more spatially extended and the dispersion of the corresponding bands is accordingly greater. The  $5\sigma$  dispersion, for example, at  $\Theta = 0.5, 0.58$ , and  $0.8$  is 0.33, 0.53, and 2.0 eV, respectively. In the experiment a certain degree of dispersion is detected for the composite  $5\sigma + 1\pi$  level, but it is not possible to decompose it into its component bands. Furthermore, the extent of the

dispersion is smaller than indicated by the present band-structure calculations and shows the need to account more fully for the interaction with the substrate.

## II. CALCULATIONAL METHOD

Our calculations were performed non-self-consistently using the first-principles [linear combination of atomic orbitals (LCAO)] extended-tight-binding (ETB) method.<sup>7</sup> Here, the wave functions of the system are expanded in terms of Bloch sums constructed out of Gaussian-type basis sets. We have used basis sets of better than double  $\zeta$  quality. These were obtained<sup>8</sup> by contracting nine  $s$  and five  $p$  atomic functions to (4,3) for both C and O and adding a single  $d$  function (exponent = 1.0).<sup>9</sup> The exponents and contraction coefficients for the  $s$  and  $p$  orbitals are given in Table I. The crystal potential was generated in the overlapping atomic potential (OAP), as well as overlapping atomic-charge-density (OAC) approximations.<sup>10,11</sup> In both cases, self-consistent atomic Hartree-Fock charge densities have been used in conjunction with the statistical exchange<sup>12</sup> approximation. The potential matrix elements were calculated in mixed direct and momentum spaces to convergence. All overlap integrals of magnitude greater than  $10^{-7}$  were retained. The calculations were performed using the well-known slab configuration.<sup>13</sup>

One domain of the  $c(4 \times 2)$ - $45^\circ$  structure formed by CO on Pd(100) at  $\Theta = 0.5$  is depicted in Fig. 1. If all CO molecules are equivalent then bridging sites of twofold symmetry must be occupied.<sup>6</sup> Such a structure model is supported by ir-reflection-absorption measurements.<sup>14</sup> Increasing the coverage results in a uniaxial compression in each of the two orthogonal domains along one of the [100] azimuthal directions. At a coverage of  $\Theta = 0.58$  the layer has a hexagonal structure (see Fig. 1) and the compression continues up to the saturation coverage of  $\Theta \sim 0.8$ . Clearly the half-coverage situation corresponds to a two-dimensional lattice characterized by the translation vectors  $\vec{\tau}_1 = a(1, 0)$  and  $\vec{\tau}_2 = a(\frac{1}{2}, 1)$ , where  $a = 7.3321$  a.u. is the lattice constant for bulk palladium. A value of 2.13 a.u. is used for the CO bond length. At higher coverages the uniaxial compression leads to translation vectors  $\vec{\tau}_1 = a(1, 0)$  and  $\vec{\tau}_2 = a(\frac{1}{2}, \lambda)$ , where  $\lambda$  is a coverage dependent parameter. For a given  $\lambda$  the coverage is given by  $\Theta = \frac{1}{2}\lambda$ . Therefore, the three coverages  $\Theta = 0.5$ , 0.58, and 0.8 depicted in Fig. 1 correspond to  $\lambda = 1$ ,  $\frac{1}{2}(3^{1/2})$ , and  $\frac{5}{8}$ , respectively. The LEED patterns obtained at these three coverages are depicted in Fig. 2, together with the appropriate surface Brillouin zones (SBZ's) of both domains. Whereas the shape of the two overlapping SBZ's varies with coverage, the directions  $\Gamma M$  and  $\Gamma K'$  are colinear. At  $\Theta = 0.8$

TABLE I. Exponents and contraction coefficients for the CO basis sets.

No.	Type	Carbon		Oxygen	
		Exponent	Coefficient	Exponent	Coefficient
1	s	5 240.635 2	0.000 937	10 662.285	0.000 799
		782.204 8	0.007 228	1 599.709 7	0.006 153
		178.350 83	0.036 344	364.725 26	0.031 157
		50.815 942	0.130 600	103.651 79	0.115 96
		16.823 562	0.318 931	33.905 805	0.301 552
2	s	6.175 776	0.438 742	12.287 469	0.444 870
		2.418 049	0.214 974	4.756 803	0.243 172
3	s	0.511 900	1.0	1.004 271	1.0
4	s	0.156 590	1.0	0.300 686	1.0
5	p	18.8418	0.013 887	34.856 463	0.015 648
		4.159 24	0.086 279	7.843 131	0.098 197
		1.206 71	0.288 744	2.308 269	0.307 748
6	p	0.385 54	1.0	0.723 164	1.0
7	p	0.121 94	1.0	0.214 882	1.0

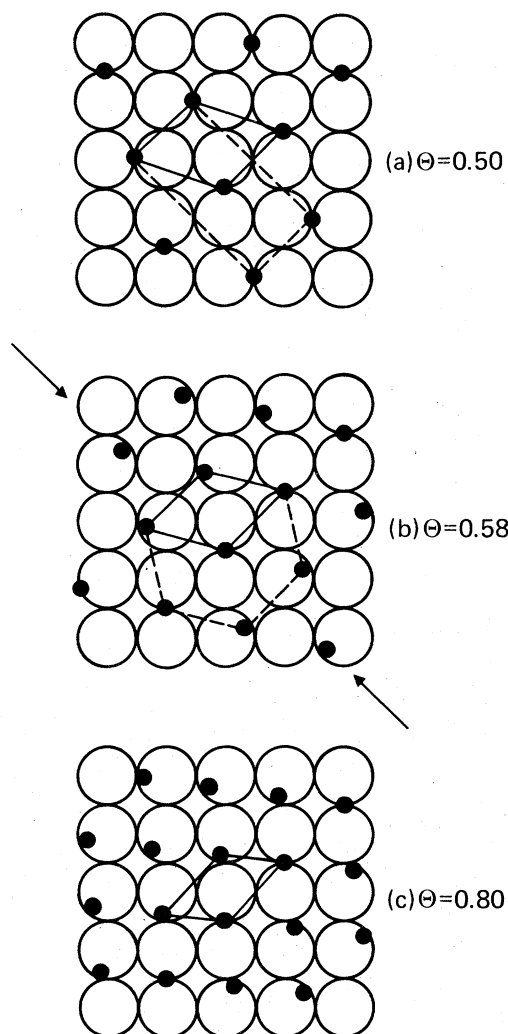


FIG. 1. Structure models for the ordered overlayers formed by CO on a Pd(100) surface between  $\Theta=0.5$  and  $\Theta=0.8$ . The arrows represent the direction of uniaxial compression of the unit cell along the [100] azimuthal direction. Only one of the two orthogonal domains is shown in each case. The primitive unit cells of the equivalent isolated adlayer are shown with solid lines.

the points  $M$  and  $K'$  are also nearly coincident. The direction  $\Gamma H$ , which is not a symmetry direction, is unique in that it is common to both SBZ's. We have calculated the band structure along various directions of the SBZ at the three coverages.

### III. EXPERIMENTAL

All measurements were performed with an ADES 400 ultrahigh vacuum electron spectrometer from VG Scientific Ltd. After bake-out pressures of typically

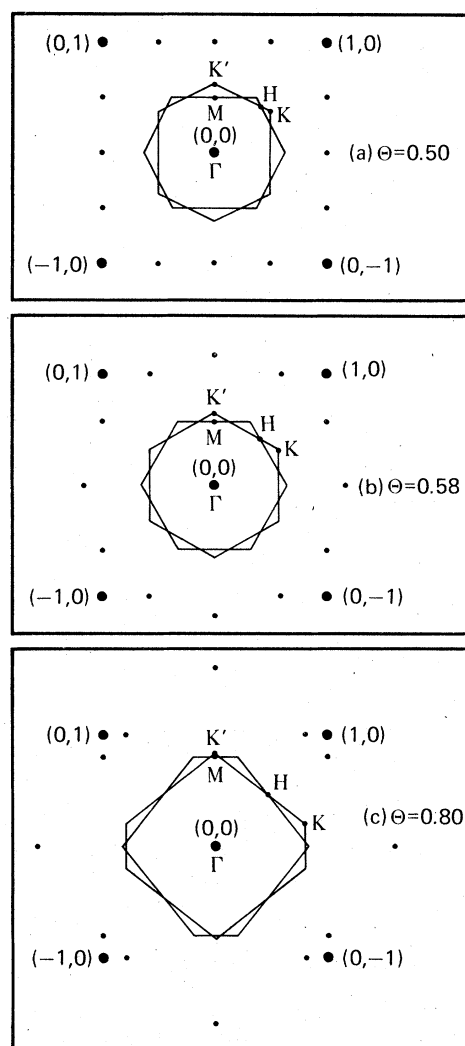


FIG. 2. LEED patterns from the two orthogonal domains of the CO-Pd(100) system at (a)  $\Theta=0.5$  [the  $c(4 \times 2)$ - $45^\circ$  structure], (b)  $\Theta=0.58$  (the hexagonal structure), and (c)  $\Theta=0.8$  ( $\sim$  saturation coverage). The patterns thus correspond to the models of the overlayers presented in Fig. 1. The weak multiple diffraction features are not shown. The respective superimposed surface Brillouin zones (SBZ's) for the two domains are also given for each coverage.

$(2-3) \times 10^{-11}$  Torr were attained. The chamber contained a windowless uv discharge lamp, an ion bombardment gun, LEED optics, Auger electron gun, and a crystal manipulator. The instrument allowed independent setting of photon angle of incidence and electron emission angle. The analyzer acceptance window was situated in the plane of incidence of the light beam. For the coverage dependence of CO adsorption on Pd(100) shown in Fig. 3 ( $\hbar\omega = 40.8$  eV) the hemispherical electron energy analyzer was operated at a pass energy of 10 eV corresponding to

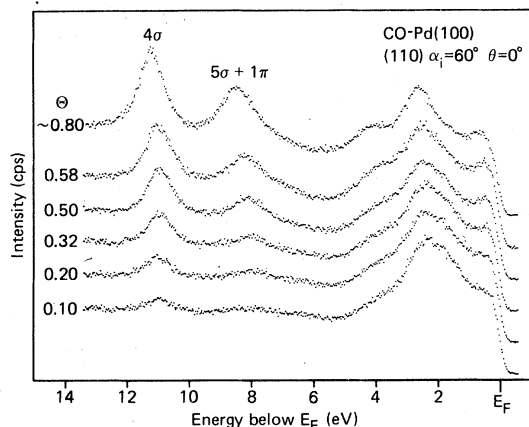


FIG. 3. Coverage dependence of CO adsorption on Pd(100) in photoemission with  $\hbar\omega = 40.8$  eV, angle of incidence,  $\alpha_i = 60^\circ$ , and normal emission ( $\theta = 0^\circ$ ).

an energy resolution of  $\sim 200$  meV. For the dispersion investigation only restricted regions of the spectrum were recorded around each adsorbate induced level, so as to improve the signal-to-noise ratio and thus the accuracy of determining the peak position. The latter could be estimated to  $\pm 40$  meV for the  $4\sigma$  peak and  $\pm 70$  meV for the composite  $1\pi/5\sigma$  peak. The parallel component of the wave vector was related to the polar angle of emission  $\theta$ , by  $k_{\parallel} = (2mE)^{1/2} \sin\theta/\hbar$ .  $E$  is the kinetic energy of the emitted electron relative to the vacuum level.

The palladium surface was cut to the desired orientation from a Marz grade single crystal supplied by Materials Research Corporation. The resulting elliptical disc was then reoriented on a polishing jig to better than  $\frac{1}{2}^\circ$  of the (100) plane and subsequently polished with successively finer diamond pastes down to  $0.25 \mu\text{m}$ . The crystal was then mounted on a holder which allowed it to be cooled to 80 K (or lower if liquid helium is used) while retaining an azimuthal movement of  $70^\circ$ . After repeated cycles of argon-ion bombardment and short anneals at  $800^\circ\text{C}$  the main impurities (sulphur, phosphorous, and carbon as detected by Auger spectroscopy) were removed. The presence of the ordered CO overlayer was established by LEED.

#### IV. RESULTS AND DISCUSSION

Figure 4 shows the band structure for the CO monolayer at  $\Theta = 0.5$  calculated using the OAP approximation with the exchange parameter  $\alpha = \frac{2}{3}$ . The  $4\sigma$  band dispersion is extremely small ( $\approx 0.02$  eV), while the  $5\sigma$  dispersion ( $\sim 0.33$  eV) and the  $1\pi$  dispersion ( $\sim 0.18$  eV) are somewhat larger. This suggests that the CO molecules at this coverage are only slightly perturbed by the intermolecular interac-

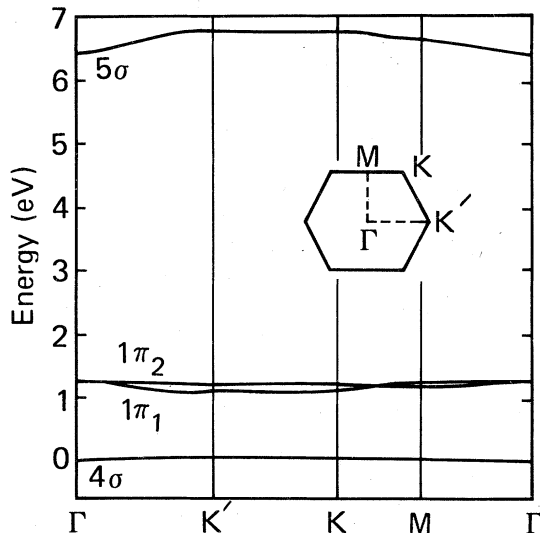


FIG. 4. Band structure of an isolated CO layer corresponding to a coverage of  $\Theta = 0.5$  on the Pd(100) surface and using the OAP approximation (see text).

tion. The fact that the  $5\sigma$  and  $1\pi$  dispersions are larger than the  $4\sigma$  dispersion is a consequence of the  $5\sigma$  and  $1\pi$  orbitals being spatially more extended than  $4\sigma$ .<sup>15</sup> The results for the hexagonal CO monolayer structure ( $\Theta = 0.58$ ) are similar. Dispersions of the  $4\sigma$ ,  $1\pi$ , and  $5\sigma$  bands increased somewhat and were found to be 0.04, 0.25, and 0.53 eV, respectively. Repeating the calculation for the saturation coverage ( $\Theta = 0.8$ ), we obtained values of about 0.3, 1.0, and 2.0 eV. As shown below, the dispersion and shape of the  $4\sigma$  band agrees well with our experimental data. However, the calculated relative separation between the  $4\sigma$  and  $1\pi$  one-electron eigenvalues at  $\Theta = 0.5$  and 0.58 is about 1.3 eV at  $\Gamma$ . Since at these coverages CO molecules in different unit cells interact rather weakly, we might expect this separation to correspond to the difference in ionization potentials (IP) for the  $4\sigma$  and  $1\pi$  levels in the free molecule. In fact the 1.3 eV calculated separation is lower than the IP difference of 2.8 eV.<sup>16</sup> The agreement between the experimental  $5\sigma$  and  $4\sigma$  ionization potential difference (5.7 eV) and the calculated separation of the eigenvalues (6.5 eV) is somewhat better. It was nonetheless felt necessary to repeat all calculations by generating the monolayer potential in a somewhat better approximation, namely, the OAC approximation.

We first performed the OAC approximation ( $\alpha = \frac{2}{3}$ ) calculations for  $\Theta = 0.58$  and found that the relative separation between  $4\sigma$  and  $1\pi$  increased to 2.6 eV at  $\Gamma$ . The average relative separation between  $4\sigma$  and  $5\sigma$  dropped significantly to 5.1 eV. These values are in reasonable agreement with the experi-

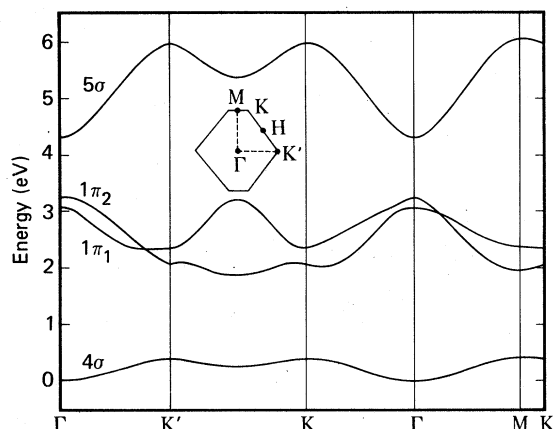


FIG. 5. Band structure of an isolated CO layer corresponding to a coverage of  $\Theta=0.8$  on the Pd(100) surface and using the OAC approximation (see text).

mental ionization potential difference for free CO. The dispersions of the  $4\sigma$ ,  $1\pi$ , and  $5\sigma$  bands were found to be 0.07, 0.27, and 0.54 eV, respectively. Clearly, these values do not change appreciably on going from the OAP to the OAC approximation.

Figure 5 shows the complete band structure for a CO monolayer at saturation coverage ( $\Theta=0.8$ ) generated using the OAC approximation with  $\alpha = \frac{2}{3}$ . Atomic localization and orbital composition of various bands at the  $\Gamma$  point are presented in Table II. The population values are quite similar to those obtained for a free CO molecule<sup>15</sup> using an identical basis set. One notes in Fig. 5 that  $\sigma$  bands have their lowest eigenvalue at  $\Gamma$  because  $s$  and  $p_z$  orbitals in different unit cells form bonding combinations at this point. Since  $\pi$  orbitals form antibonding combinations, these bands have their highest eigenvalues at  $\Gamma$ . In the free CO molecule the  $1\pi$  orbitals are dou-

bly degenerate. Due to the low symmetry of the SBZ this degeneracy is removed, even at the  $\Gamma$  point which has  $C_{2v}$  symmetry. The calculation shows that the  $1\pi_1(p_x)$  band at  $\Gamma$  has a slightly lower energy than the  $1\pi_2(p_y)$  band. The band dispersions of  $4\sigma$ ,  $1\pi$ , and  $5\sigma$  were found to be 0.4, 1.4, and 1.7 eV, respectively.

Kasowski<sup>17</sup> has performed CO adlayer calculations at three symmetry points in the SBZ corresponding to the  $c(2 \times 2)$  CO overlayer on Ni(100). He obtains a  $4\sigma$  band width of  $\sim 0.32$  for the isolated layer and  $\sim 0.43$  eV when four layers of Ni substrate are included. Although the absolute coverage is lower for  $\Theta=0.5$  on Ni(100) than for  $\Theta=0.8$  on Pd(100) his dispersion is almost identical to that obtained in the present calculation. However, for the isolated layer, his band dispersion presents an unphysical picture in that the  $4\sigma$  eigenvalue does not have its lowest value at the  $\Gamma$  point. It is also strange that in his calculation the  $4\sigma$  band width (which is a measure of the extent of dispersion) increases through the action of the substrate, whereas the  $5\sigma$  and  $1\pi$  band widths are little affected.

We also examined the sensitivity of the eigenvalue spectrum to the choice of the exchange parameter  $\alpha$ . The results for three different values of  $\alpha$  are summarized in Table III. The value, 0.75, is the optimized  $\alpha$  given by Schwarz.<sup>18</sup> From the table, it is clear that the widths of all the bands decrease somewhat with the increasing value of  $\alpha$ . However, the shape of the bands is relatively insensitive to the particular choice of  $\alpha$ . We can similarly argue that the incorporation of self-consistency would not essentially alter the conclusions.

Experimental and theoretical studies have shown that the  $4\sigma$  orbital of an isolated CO molecule is not substantially affected by chemisorption on a metal surface. It is therefore quite reasonable to compare the dispersion of this band obtained in the present

TABLE II. Atomic localization and orbital composition (in percent) of the Bloch sums for the eigenstates<sup>a</sup> at the  $\Gamma$  point ( $\vec{k}_{\parallel}=0$ ) for CO monolayer at  $\Theta=0.8$  and  $\alpha = \frac{2}{3}$ .

State	$E$ (eV)	Atomic localization		Orbital composition <sup>b</sup>			
		C	O	$s$	$p_x$	$p_y$	$p_z$
$4\sigma$	0.00	18	82	40	0	0	60
$1\pi_1$	3.06	24	76	0	99	0	0
$1\pi_2$	3.24	23	77	0	0	99	0
$5\sigma$	4.31	94	6	64	0	0	36
$2\pi_1^*$	13.68	77	23	0	99	0	0
$2\pi_2^*$	13.97	78	22	0	0	99	0

<sup>a</sup>All eigenvalues are measured with respect to  $4\sigma$ .

<sup>b</sup>All  $\pi$  states contain 1%  $d$  character.

TABLE III. Energy eigenvalues<sup>a</sup> (eV) at  $\Gamma$  and  $M$  for CO monolayer at  $\Theta=0.8$  for several values of the exchange parameter  $\alpha$ .

State	$\alpha=0.67$		$\alpha=0.75$		$\alpha=0.80$	
	$\Gamma$	$M$	$\Gamma$	$M$	$\Gamma$	$M$
$4\sigma$	0.00	0.42	0.00	0.33	0.00	0.28
$1\pi_1$	3.06	1.96	3.04	2.12	3.04	2.21
$1\pi_2$	3.24	2.38	3.19	2.47	3.17	2.52
$5\sigma$	4.31	6.05	5.02	6.63	5.48	7.00
$2\pi_1^*$	13.68	11.59	14.02	12.15	14.24	12.50
$2\pi_2^*$	13.97	12.44	14.28	12.90	14.48	13.20

<sup>a</sup>All eigenvalues are measured with respect to the value of  $4\sigma$  at  $\Gamma$ .

calculations for an isolated layer with angular-resolved photoemission data from the CO-Pd(100) system. This has been done in Fig. 6 for three different  $\bar{k}_{||}$  directions at  $\theta=0.8$ . Photoemission measured in any one azimuthal direction will be the sum of emission from the two orthogonal domains present on the surface. It can be assumed that each is present in equal amounts. Thus in the [100] azimuthal direction of the crystal, we will observe superimposed emission from points along  $\Gamma M$  and  $\Gamma K'$ . Only along the unique  $\Gamma H$  direction (corresponding to [110]) is it possible to measure along a direction common to both domains. Not only might we expect experimentally different degrees of dispersion between the [100] and [110] directions but also maxima at different  $\bar{k}_{||}$  (or, alternatively, at different polar emission angles), because the distance to the zone edge is considerably shorter along  $\Gamma H$ . Reference to Fig. 6 shows that this is indeed observed in practice. Furthermore, the maxima in the dispersion curves occur at those values of  $\bar{k}_{||}$  corresponding to the zone edge, which in turn can be derived independently from LEED data. The comparison of theory and experiment for the  $\Gamma H$  directions in Fig. 6(a) show that agreement is better for the OAC approximation (full line) than for the OAP approximation (dotted line). In Figs. 6(b) and 6(c) are shown the theoretical dispersions for the  $\Gamma M$  and  $\Gamma K'$  directions, respectively. As noted above, these directions cannot be separated experimentally and in each case the measured points correspond to the combined direction  $\Gamma M + \Gamma K'$ . Good agreement between experiment and theory is obtained until the zone edge is reached. At this point emission from  $M\Gamma$  in the second SBZ appears to dominate over emission from  $K'MK'\Gamma$  in the other orthogonal SBZ. The data points of Fig. 6 were taken in the incidence plane with the analyzer on the opposite side of the surface normal from the light source. The same dispersion effect was observed when the analyzer was positioned in the avail-

able range of polar angles,  $\theta$ , on the same side.

Although the present theory is unlikely to account satisfactorily for the dispersion of the  $1\pi$  and  $5\sigma$  levels because of their stronger interaction with the substrate, it is still worthwhile examining the experimental data. In Fig. 7 we show the dispersion of the combined  $5\sigma + 1\pi$  level in the direction  $\Gamma M$  ( $\Gamma K'$ ) and  $\Gamma H$  at  $\Theta=0.8$ . The theory predicts that the  $1\pi$  and  $5\sigma$  bands should disperse strongly away from  $\Gamma$  in opposite directions, which might be expected to lead to substantial peak broadening particularly near the zone edge. Instead, virtually no change in half-width is observed experimentally and the position of the peak maximum changes by only 0.2–0.3 eV (Fig. 7). We are, however, still dealing with some kind of dispersion effect, because the maxima in each direction coincide with the edge of the SBZ. The fact that the predicted effects are not observed in practice is due to the neglect of the substrate in the present calculation: only the direct through-space lateral interaction is considered. It is possible nonetheless to present some qualitative arguments which account for the observed behavior. From experiments with polarized HeI radiation at  $\Theta=0.5$  and normal emission we have determined that the  $5\sigma$  level lies at 0.4 (0.2) eV further below  $E_F$  than the  $1\pi$  level. Due to problems with the background, it was not possible to achieve this separation at  $\Theta=0.8$ , but it is reasonable to assume that the same applies at the  $\Gamma$  point in the high coverage situation. On the basis of the present calculation the consequence would be a crossing of the  $5\sigma$  and  $1\pi$  bands. In the mirror planes  $\Gamma M$  and  $\Gamma K'$  the  $5\sigma$  band would hybridize with one of the two  $1\pi$  bands, which could substantially reduce the extent of dispersion. The other  $1\pi$  band can only be excited by the  $s$  component of the incident radiation and will not appear so strongly in the spectrum. Along a general direction in the SBZ such as  $\Gamma H$ , the  $5\sigma$  band will hybridize with both  $1\pi$  bands. Depending on the strength of the interaction the hybridiza-

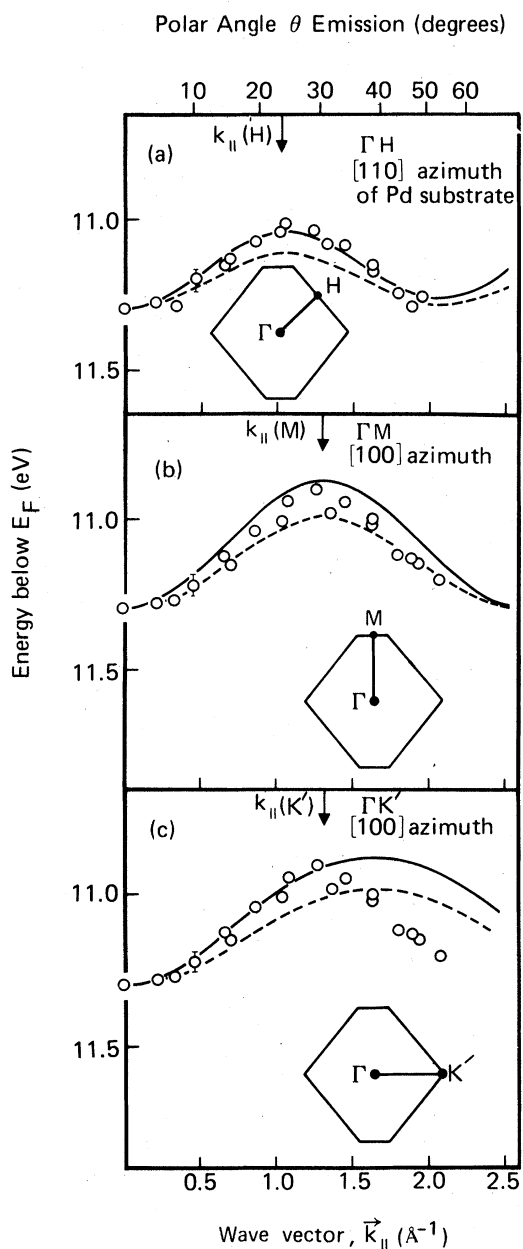


FIG. 6. Comparison of calculated  $4\sigma$  band dispersion along (a)  $\Gamma H$ , (b)  $\Gamma M$ , and (c)  $\Gamma K'$  with angular resolved photoemission data. Solid line: OAC; dashed line: OAP; points: experimental data at  $\hbar\omega = 40.8$  eV and  $\alpha_i = 60^\circ$ . The error bar, representing an inaccuracy of determination of the peak maximum of  $\pm 0.04$  eV, applies to all points.

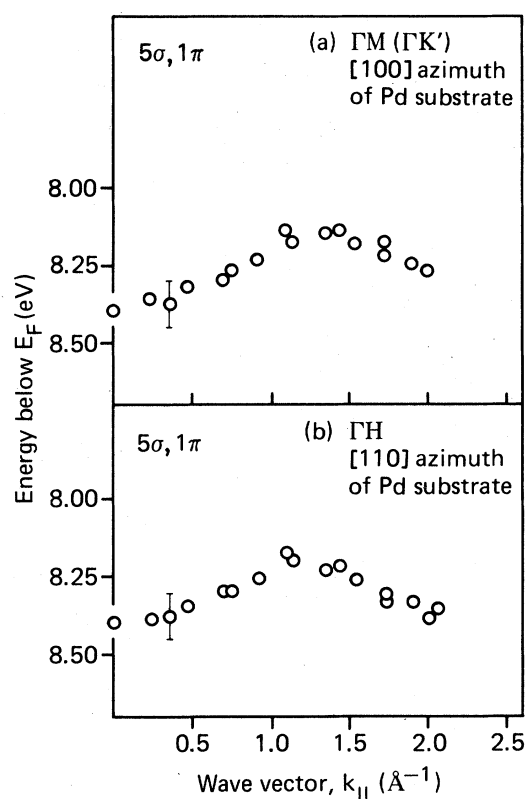


FIG. 7. Experimental dispersion of the peak maximum of the combined  $1\pi$ ,  $5\sigma$  level along (a)  $\Gamma M$  ( $\Gamma K'$ ) and (b)  $\Gamma H$  at  $\hbar\omega = 40.8$  eV and  $\alpha_i = 60^\circ$ . The error bar, representing an inaccuracy of determination of the peak maximum of  $\pm 0.07$  eV, applies to all points.

tion could therefore lead to three, in the spectrum overlapping, bands with only a small variation in separation throughout the SBZ. This would correspond to the observed result.

We conclude by noting that much of the dispersion observed in the  $4\sigma$  band for CO-Pd(100) at high coverage can be accounted for by the direct CO-CO lateral interaction. For those orbitals of an adsorbed molecule, which are strongly involved in the chemisorption bond, the isolated adlayer calculation is not expected to be adequate for describing dispersion. Substrate effects must be treated explicitly. In the case of palladium LCAO first-principle calculations are not possible at the present time. On the other hand, because of the high degree of ordering in the adlayer, the CO-Pd(100) system is particularly suitable for demonstrating experimentally adsorbate band formation.

- \*Permanent address: Institute für Theoretische Physik B, TU Clausthal, 3392 Clausthal-Zfd, West Germany
- <sup>1</sup>K. Horn, M. Scheffler, and A. M. Bradshaw, *Phys. Rev. Lett.* **41**, 822 (1978); M. Scheffler, K. Horn, A. M. Bradshaw, and K. Kambe, *Surf. Sci.* **80**, 69 (1979).
- <sup>2</sup>P. K. Larsen, N. V. Smith, M. Schlüter, H. H. Farrell, K. M. Ho, and M. L. Cohen, *Phys. Rev. B* **17**, 2612 (1978).
- <sup>3</sup>K. Jacobi and C. V. Muschwitz, *Solid State Commun.* **26**, 477 (1978).
- <sup>4</sup>K. Horn, A. M. Bradshaw, K. Hermann, and I. P. Batra *Solid State Commun.* (to be published).
- <sup>5</sup>See for example, I. P. Batra and P. S. Bagus, *Solid State Commun.* **16**, 1097 (1975); T. Gustafson, E. W. Plummer, D. E. Eastman, and J. L. Freeouf, *Solid State Commun.* **17**, 391 (1975); C. L. Allyn, T. Gustafsson, and E. W. Plummer, *Chem. Phys. Lett.* **47**, 127 (1977).
- <sup>6</sup>J. C. Tracy and P. W. Palmberg, *J. Chem. Phys.* **51**, 4852 (1969).
- <sup>7</sup>For details see I. P. Batra, S. Ciraci, and W. E. Rudge, *Phys. Rev. B* **15**, 5858 (1977), and references therein.
- <sup>8</sup>F. B. Diujneveldt, IBM Research Report No. RJ 945 (unpublished); C. P. Keijzers, P. S. Bagus, and J. P. Worth (unpublished); See also Ref. 15.
- <sup>9</sup>Following B. Roos and P. Siegbahn, *Theor. Chim. Acta* **17**, 199 (1970).
- <sup>10</sup>See for example, F. Herman, R. L. Kortum, C. D. Kuglin, and J. P. Van Dyke, in *Methods in Computational Physics*, edited by B. J. Alder (Academic, New York, 1968), Vol. VIII., p. 193.
- <sup>11</sup>C. S. Wang and J. Callaway, *Phys. Rev. B* **15**, 298 (1977); A. Zunger and A. J. Freeman, *Phys. Rev. B* **15**, 4716 (1977).
- <sup>12</sup>J. C. Slater, *Phys. Rev.* **81**, 385 (1951); W. Kohn and L. J. Sham, *Phys. Rev.* **140**, A1133 (1965); J. C. Slater and J. H. Wood, *Int. J. Quantum Chem.* **45**, 3 (1971).
- <sup>13</sup>K. Hirabayashi, *J. Phys. Soc. Jpn.* **27**, 1475 (1969); G. P. Alldredge and L. Kleinman, *Phys. Rev. Lett.* **28**, 1264 (1972) and *Phys. Rev. B* **10**, 559 (1974); R. V. Kasowski, *Phys. Rev. Lett.* **33**, 1174 (1974); J. G. Gay, J. R. Smith, and F. J. Arlinghaus, *Phys. Rev. Lett.* **38**, 561 (1977); I. P. Batra and S. Ciraci, *Phys. Rev. Lett.* **39**, 774 (1977); G. S. Painter, *Phys. Rev. B* **17**, 3848 (1978); C. S. Wang and A. J. Freeman, *Phys. Rev. B* **19**, 793 (1979).
- <sup>14</sup>A. M. Bradshaw and F. M. Hoffmann, *Surf. Sci.* **72**, 513 (1978).
- <sup>15</sup>P. S. Bagus and K. Hermann, *Solid State Commun.* **20**, 5 (1976); K. Hermann and P. S. Bagus, *Phys. Rev. B* **16**, 4195 (1977); P. S. Bagus (unpublished).
- <sup>16</sup>D. W. Turner, C. Baker, A. D. Baker, and C. R. Brundle, *Molecular Photoelectron Spectroscopy* (Interscience, New York, 1970).
- <sup>17</sup>R. V. Kasowski, *Phys. Rev. Lett.* **37**, 219 (1976).
- <sup>18</sup>K. Schwarz, *Phys. Rev. B* **5**, 2466 (1972).